The Astrophysical Journal, 757:71 (7pp), 2012 September 20 doi:10.1088/0004-637X/757/1/71

IMPACT OF A REALISTIC DENSITY STRATIFICATION ON A SIMPLE SOLAR DYNAMO CALCULATION

Elisa Cardoso[1,2] and Ilídio Lopes[1,2]
[1] Centro Multidisciplinar de Astrofísica, Instituto Superior Técnico, Av. Rovisco Pais, 1049-001 Lisboa, Portugal; ilidio.lopes@ist.utl.pt
[2] Departamento de Física, Universidade de Évora, Colégio António Luis Verney, 7002-554 Évora, Portugal
Received 2012 May 17; accepted 2012 July 25; published 2012 September 5

ABSTRACT

In our Sun, the magnetic cycle is driven by the dynamo action occurring inside the convection zone, beneath the surface. Rotation couples with plasma turbulent motions to produce organized magnetic fields that erupt at the surface and undergo relatively regular cycles of polarity reversal. Among others, the axisymmetric dynamo models have been proved to be a quite useful tool to understand the dynamical processes responsible for the evolution of the solar magnetic cycle and the formation of the sunspots. Here, we discuss the role played by the radial density stratification on the critical layers of the Sun on the solar dynamo. The current view is that a polytropic description of the density stratification from beneath the tachocline region up to the Sun's surface is sufficient for the current precision of axisymmetric dynamo models. In this work, by using an up-to-date density profile obtained from a standard solar model, which is itself consistent with helioseismic data, we show that the detailed peculiarities of the density in critical regions of the Sun's interior, such as the tachocline, the base of the convection zone, the layers of partial ionization of hydrogen and helium, and the super-adiabatic layer, play a non-negligible role on the evolution of the solar magnetic cycle. Furthermore, we found that the chemical composition of the solar model plays a minor role in the formation and evolution of the solar magnetic cycle.

Key words: magnetic fields – Sun: general – Sun: helioseismology – Sun: interior – sunspots

Online-only material: color figures

1. INTRODUCTION

The modeling of the Sun and its magnetic activity has been a challenge that astrophysicists and solar physicists have been addressing with a certain degree of success. The interest and motivation is to better understand the evolution of our star, not only to answer to fundamental questions about the physical mechanisms operating in the interior of the Sun, but also to explore the possibility that, in the near future, we will be able to follow the Sun's irregular magnetic activity. Ultimately, the solar activity that regulates the space weather has a non-negligible impact on Earth's atmosphere and climate (e.g., Charbonneau 2010).

In the past 40 years, a tremendous advance has been made in the comprehension of the mechanisms occurring in the Sun's interior, namely, the basic macroscopic structure of the solar interior (Turck-Chieze & Couvidat 2011) as well as the dynamic processes occurring in the different layers of the Sun (e.g., Howe 2009). Most of this progress is due to the field of helioseismology, as well as solar neutrinos. The success of the modeling of the solar interior has culminated in the definition of the so-called standard solar model (e.g., Turck-Chieze & Lopes 1993; Turck-Chieze & Couvidat 2011). Nevertheless, there is still a major challenge to answer about the solar interior. What are the physical mechanisms regulating the solar cycle and magnetic activity? In recent years, an important effort was done to try to understand such mechanisms, in particular the role played by the magnetic field transport on the evolution of the solar magnetic cycle.

The modeling of the solar magnetic cycle has been approached through different perspectives, among the different studies of the solar dynamo, the so-called kinematic mean-field axisymmetric model is very likely the most common and successful method used to model the solar magnetic cycle (e.g., Charbonneau 2010). This model is one of the best tools to understand solar observations and to test the more advanced dynamo flux-transport simulations. Kinematic dynamo models have been quite successful in reproducing many of the characteristics of the solar magnetic cycle (e.g., Dikpati & Choudhuri 1995; Choudhuri et al. 1995; Durney 1997; Dikpati & Charbonneau 1999; Nandy & Choudhuri 2001; Rempel 2006; Guerrero & de Gouveia Dal Pino 2008; Muñoz-Jaramillo et al. 2009, 2011). By using a one-dimensional dynamo model as a diagnostic tool of the axisymmetric models, Lopes & Passos (2009) have succeeded in reproducing some of the main observational characteristics of the Sun's spot data, including the impact that fluctuations on the amplitude and frequency of the meridional flow have on the strength of the solar cycle (Passos & Lopes 2012).

Among others, Muñoz-Jaramillo et al. (2010), Chatterjee et al. (2004), Yeates et al. (2008), and Nandy & Choudhuri (2002) have been quite successful in including the meridional circulation and differential rotation obtained from the helioseismology data in the kinematic dynamo models. These types of studies have shown that the structure and strength of the meridional circulation determines the duration of the magnetic cycle, the rising of magnetic tube fluxes, and the strength and the polarity reversal of the magnetic field (Yeates et al. 2008; Hathaway 2011). Helioseismology has succeeded in detecting the meridional flow near the surface (Haber et al. 2002; Zhao & Kosovichev 2004). However, the meridional return flow near the base of the convective zone proposed by various theoretical dynamo models (Dikpati & Charbonneau 1999; Chatterjee et al. 2004; Guerrero & de Gouveia Dal Pino 2008; Bonanno et al. 2002) has not been observed up to now.

Several authors have tried to determine the effective role and the efficiency of the meridional circulation in the evolution of the magnetic field (e.g., Dikpati & Gilman 2012; Dikpati & Charbonneau 1999), namely, the meridional circulation influence on the polar magnetic field at the surface. Although, the

large motions of fluids presently being included in the solar dynamos have an important impact on the evolution of the magnetic field, the polytropic density stratification usually assumed can significantly mask the contribution of such dynamical effects.

In this work, we follow a similar strategy to the previous authors that attempt to include the helioseismology data in the kinematic dynamo models (Chatterjee et al. 2004; Yeates et al. 2008; Nandy & Choudhuri 2002), but our work will be focused on testing a density profile consistent with helioseismology data. Using a publicly available solar dynamo code, we have tested the impact of the radial density profile obtained from the standard solar model (e.g., Turck-Chieze & Lopes 1993) on this type of dynamo model. The solar density profile is in itself consistent with helioseismic data. In this work, we propose a methodology to include such a density profile in these types of solar dynamo models, and discuss the implications of such modification on the behavior of the solar magnetic cycle.

In the next section, we describe the current status of the solar standard model and its consistency with helioseismology data. In Section 3, we detail the basic features of the kinematic axisymmetric model, which we refer to as the reference dynamo model for which we consider the usual standard parameterization. In Section 4, we describe the methodology for using the helioseismic consistent radial density profile and discuss its impact on the meridional circulation. In Section 5, we report the new dynamo simulations and discuss the results in terms of the butterfly diagram. In Section 6, we comment on the main results using this improved helioseismic density profile, and discuss the impact of such results for solar standard modeling and solar dynamo models alike.

2. HELIOSEISMOLOGY AND THE SOLAR STANDARD MODEL: THE CRITICAL LAYERS

The present seismic data allow the determination of the sound speed and density to be obtained from the surface up to 6% of the solar radius (Basu et al. 2009; Turck-Chieze et al. 1997). Although for above 98% of the solar radius the inversion of sound speed and density profiles cannot be done reliably, mainly due to the complex interaction of acoustic waves with the upper layers of the star (Lopes & Gough 2001), by comparing the solar standard model with the helioseismic data, we found that the sound speed difference is of the order of 2% (in most of the radiative region), and the density difference is of the order of 10% (in the convective zone). These differences in the envelope of the star are mainly due to the uncertainties in the microscopic physics of the solar standard model, as well as uncertainties on the physical processes related to turbulent convection, acoustic pulsation, and magnetic activity. Indeed, the dynamics of the physical processes occurring in the upper layers of the star, related to the magnetic activity and convection, are quite complex and some of their effects can be observed in the acoustic spectrum of oscillations (Rosenthal et al. 1995, 1999; Nordlund et al. 2009).

Another illustration of the uncertainty of the standard solar model is the well-known composition problem, where the new surface measurements of abundances of the chemical elements, carbon, nitrogen, and oxygen have increased the difference between the sound speed profile of the solar standard model and the sound speed obtained from helioseismology.

Figure 1 shows the profile of the sound speed and density of the solar standard model computed using the CESAM evolution code (Morel 1997) for the GS98 abundance composition (Grevesse & Sauval 1998). This solar model is used as a reference in this work. Nevertheless, for completeness, we have also calculated the solar standard model using the new AGS05 abundance composition (Asplund et al. 2005). Our version of stellar evolution has an up-to-date refined microscopic physics (updated equation of state, opacities, nuclear reactions rates, and an accurate treatment of microscopic diffusion of heavy elements), including the solar mixture of Asplund et al. (2005, 2009) or Grevesse & Sauval (1998). All the solar models are calibrated to the present solar radius $R_\odot = 6.9599 \times 10^{10}$ cm, luminosity $L_\odot = 3.846 \times 10^{33}$ erg s^{-1}, mass $M_\odot = 1.989 \times 10^{33}$ g, and age $t_\odot = 4.54 \pm 0.04$ Gyr (e.g., Turck-Chieze & Couvidat 2011). The models are required to have a fixed value of the photospheric ratio $(Z/X)_\odot$, where X and Z are the mass fraction of hydrogen and the mass fraction of elements heavier than helium. The value of $(Z/X)_\odot$ is determined according to the solar mixture proposed. Our reference model is a standard solar model (Turck-Chieze & Lopes 1993) that shows acoustic seismic diagnostics and solar neutrino fluxes similar to other solar standard models (Guzik & Mussack 2010; Serenelli et al. 2009; Bahcall et al. 2005; Turck-Chieze et al. 2010).

The inversion of the sound speed and density profiles used in this study (cf. Figure 1) were done using the seismic data of the BISON and GONG networks (Basu et al. 2009). These seismic data are consistent with the previous high accuracy measurements done by the GOLF and MDI instruments of the *Solar and Heliospheric Observatory* mission (Turck-Chieze et al. 1997). The clearly different signature in the composition leads to a quite different structure of the upper layers, which in turn can produce an observable effect on the evolution of the solar magnetic cycle. Although the base of the convection zone is quite different between the two models, their effect on the evolution of the solar magnetic cycle seems to be quite small.

3. THE SOLAR DYNAMO: THE STANDARD CASE

The global solar cycle features observed in the Sun can be described as being produced by a solar dynamo model driven by an α-effect mechanism, described by the governing equation for the evolution of the large-scale magnetic field $\mathbf{B}$. From the mean-field electrodynamics (Moffatt 1978; Krause & Raedler 1980), the induction equation with the additional α-effect term reads

$$\frac{\partial \mathbf{B}}{\partial t} = \nabla \times (\mathbf{U} \times \mathbf{B} + \alpha \mathbf{B} - \eta \nabla \times \mathbf{B}), \quad (1)$$

where $\mathbf{U}$ is the large-scale mean flow and η is the total magnetic diffusivity (including the turbulent diffusivity and the molecular diffusivity). To a first approximation, the large-scale magnetic field in the Sun is axisymmetric about the Sun's rotation axis, and antisymmetric about the equatorial plane. This theoretical hypothesis is supported by the existence of the sunspot butterfly diagram, Hale's polarity law, and synoptic magnetograms. Therefore, the solar dynamo is usually described by a two-dimensional axisymmetric mean-field model in a spherical-shell domain such that $R_\mathrm{b} \leqslant r \leqslant R_\mathrm{t}$ and $0^\mathrm{o} \leqslant \theta \leqslant 90^\mathrm{o}$ where r, θ, and ϕ are the spherical polar coordinates. In our case, we choose $R_\mathrm{b} = 0.55\ R_\odot$ and $R_\mathrm{t} = R_\odot$, if not stated otherwise. The choice of domain is motivated by the direct numerical simulation of convective dynamos (e.g., Mitra et al. 2011). Furthermore, the dynamo is considered to be in the kinematic regime, such that the mean flow $\mathbf{U}$ is given by $\mathbf{U} = \mathbf{U}_\mathrm{circ} + \mathbf{U}_\mathrm{rot} + \mathbf{U}_\mathrm{wind}$, where $\mathbf{U}_\mathrm{circ}$ and $\mathbf{U}_\mathrm{rot}$ are, respectively, the large-scale velocity meridional

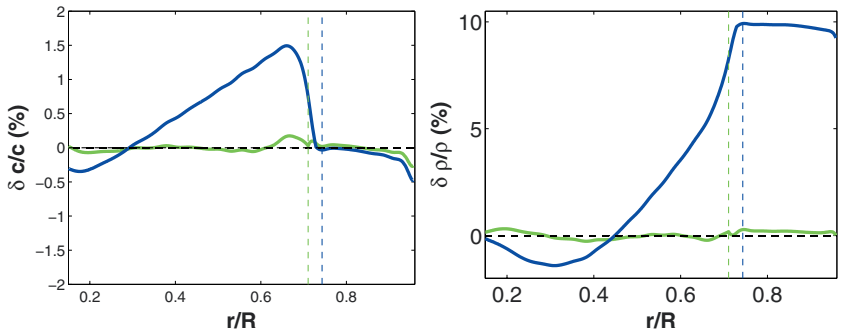

Figure 1. Comparison of the sound speed (left panel) and density (right panel) radial profiles between the solar standard model and helioseismology inverted data (Basu et al. 2009; Turck-Chieze et al. 1997). The solar structure was computed for two different solar surface chemical abundances obtained by Grevesse & Sauval (1998, GS98) and Asplund et al. (2005, AGS05). The continuous line corresponds to the AGS05 solar model and the green continuous line to the GS98 solar model. The location of the base of the convection zone is indicated by a vertical line: 0.743 $R_\odot$ (blue dashed line) for the AGS05 solar model and 0.71 $R_\odot$ (green dashed line) for the GS98 solar model. Our standard solar model is in agreement with the most current helioseismology diagnostics and other solar standard models published in the literature (Turck-Chieze & Lopes 1993; Bahcall et al. 2005; Guzik 2011; Turck-Chieze et al. 2010).

(A color version of this figure is available in the online journal.)

circulation flow and the differential rotation flow. $\mathbf{U}_{\rm wind}$ is a flow term included to take into account the effect of the solar wind in the outer region of the model through which the wind flows, but extends the outer boundary beyond the convection zone. Although $\mathbf{U}_{\rm wind}$, in general, is different from zero (at least in the case of large magnetic activity), nevertheless, we will consider its contribution to be negligible, as this term is much smaller than other components. The two other components are obtained from solar observations and helioseismology. Usually, the differential rotation is $\mathbf{U}_{\rm rot} = \Omega(r,\theta)\ r\sin\theta\ \hat{\mathbf{e}}_\phi$, and the meridional velocity $\mathbf{U}_{\rm circ} = v_r\ \hat{\mathbf{e}}_r + v_\theta\ \hat{\mathbf{e}}_\theta$ is given by

$$\rho v_r = \frac{1}{r^2\sin\theta}\frac{\partial\Psi(r,\theta)}{\partial\theta} \qquad \rho v_\theta = -\frac{1}{r\sin\theta}\frac{\partial\Psi(r,\theta)}{\partial r}, \quad (2)$$

where $\Psi(r,\theta) \equiv \psi(r,\theta) r\sin\theta$ is the meridional circulation for which $\rho\mathbf{U}_{\rm circ} = \nabla\times(\Psi\mathbf{e}_\phi)$.

In this work, we compute the evolution of $\mathbf{B}$, in the axisymmetric kinematic dynamo approximation. Consequently, the previous mean-field MHD equation (1) is written in a standard form (Chatterjee et al. 2004), resulting in a set of two coupled equations, to describe the evolution of $\mathbf{B}$. It follows that $\mathbf{B} = B(r,\theta)\mathbf{e}_\phi + \mathbf{B}_p$ where $B(r,\theta)$ and $\mathbf{B}_p = \nabla\times[A(r,\theta)\mathbf{e}_\phi]$ are known as the toroidal and poloidal components of the magnetic field. In this approximation, the solar magnetic cycle is interpreted as the result of the generation and recycling of these two components of the magnetic field.

We model the evolution of the large-scale mean magnetic field under the axisymmetric kinematic dynamo approximation by using the publicly available solar dynamo code Surya, which has been used in a multitude of applications (Nandy & Choudhuri 2002; Chatterjee et al. 2004; Choudhuri et al. 2007). This axisymmetric dynamo code is similar to others used by several authors (e.g., Charbonneau 2010).

The meridional circulation that is central to such types of dynamo models is implemented by using a stream function $\Psi(r,\theta)$ as defined in Equation (2). As usual, $\Psi(r,\theta)$ is chosen to be a single-cell meridional circulation flow. Based upon physical considerations, $\Psi(r,\theta)$ can be analytically represented (Chatterjee et al. 2004; Choudhuri et al. 2005). In this type of dynamo model (cf. Equation (2)), the density stratification is always assumed to be polytropic, such that the density $\rho_{\rm pol}(r)$ is given by

$$\rho_{\rm pol}(r) \sim (R_{\rm t}/r - \gamma)^m, \quad (3)$$

where $\gamma = 0.95$ is a constant and m is a polytropic exponent, for which the values are fixed by choosing $\rho_{\rm pol}(r)$ to be the closest to the solar standard model (as expected, m is of the order of 3/2). In the remainder of the paper, we will call the stream function $\Psi_{\rm pol}(r,\theta)$ if the density profile $\rho_{\rm pol}$ is used in the computation of the stream function. Likewise for other variables, this model will be referred to as the reference solar dynamo model.

Another quantity that plays a major role in the solar dynamo is the total magnetic diffusivity. The diffusivity regulates the strength of the toroidal and poloidal magnetic field components. This complex physical process is very significant in most of the convection zone. In this model, the total magnetic diffusivity is represented by two components (poloidal ($i = p$) and toroidal ($i = t$) components) that are radially dependent on diffusivity profiles, given by $\eta_i(r) = \eta_{\rm m} + \zeta_{im}\kappa_{i1}(r) - \zeta_{io}\kappa_{i2}(r)$, where $\kappa_{ij}(r) = 1 + {\rm erf}[(r - r_{ij})/d_s]$ (with $j = 1, 2$) and $\zeta_{ik} = (\eta_{io} - \eta_k)/2$ (with $k = {\rm m}, {\rm o}$). The parameters of the function $\kappa_{ij}(r)$ and expression ζ_{ik} are the following, $d_s = 0.025\,R_\odot$, $r_{p1} = 0.7\,R_\odot$, $r_{t1} = 0.72\,R_\odot$, and $r_{p2} = r_{t2} = 0.975\,R_\odot$. In the radiative zone, we assume only the existence of molecular diffusivity $\eta_{\rm m} = 2.2\times10^8$ cm^2 s^{-1}. At the surface, both components of the diffusivity η_p and η_t increase to high values ($\sim10^{12}$ cm^2 s^{-1}) in agreement with surface flux-transport models and observational estimates, with $\eta_{\rm o} = 2.0\times10^{12}$ cm^2 s^{-1}, $\eta_{\rm to} = 4.0\times10^{10}$ cm^2 s^{-1}, and $\eta_{\rm po} = 1.25\times10^{12}$ cm^2 s^{-1}, if not stated otherwise. This formulation is identical to Yeates et al. (2008).

In this version of the Surya code, the differential rotation profile $\Omega(r,\theta)$ that describes the differential rotation in the solar convection zone was obtained by fitting the data from helioseismology (Schou et al. 1998; Charbonneau et al. 1999). The buoyancy algorithm to model the radial transport of magnetic flux and the Babcock–Leighton α-mechanism follows the procedure described in Nandy & Choudhuri (2001), Babcock (1961), and Leighton (1969).

4. THE RADIAL DENSITY PROFILE IN THE UPPER LAYERS AND THE BASE OF THE CONVECTIVE ZONE OF THE SUN

The solar density profile, as determined by helioseismology, is the best signature of the physical processes occurring beneath the base of the convection zone, the convection zone, and the most external layers of the Sun. Helioseismology, as well as the

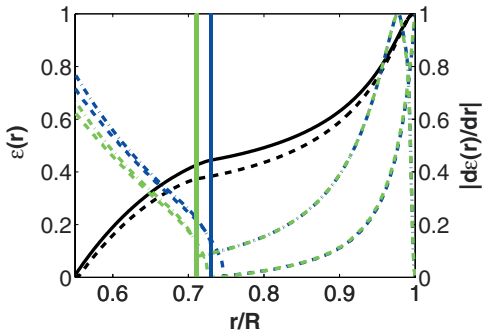

Figure 2. Variation of the function $\epsilon(r)$ and its derivative $\epsilon'(r)$ with the solar radius, $\epsilon(r)$ determines the relative difference between the radial density profile $\rho_{\rm ssm}(r)$ obtained from a solar standard model and the polytropic density profile used in the reference dynamo model $\rho_{\rm pol}(r)$, i.e., $\epsilon(r) = (\rho_{\rm ssm}(r) - \rho_{\rm pol}(r))/\rho_{\rm pol}(r)$: left axis: $\epsilon(r)$ for the AGS05 solar model (black continuous line) and the GS98 solar model (black dashed line); right axis: $|\epsilon'(r)|$ for the AGS05 solar model (blue lines) and the GS98 solar model (green lines). The two lines correspond to different dynamo models: model A with $R_{\rm t} = 0.96\ R_\odot$ (dashed line) and model E with $R_{\rm t} = R_\odot$ (dash-dotted line). It is also shown the location of the base of convection zone as indicated in Figure 1. (A color version of this figure is available in the online journal.)

standard solar model, shows an intricate radial profile of density (cf. Figure 1) which is the consequence of the complex physical processes occurring at the different regions of the solar envelope, where the dynamo produces the solar magnetic field, not only in the bulk of the convection zone but, more critically, in other regions that we know play a crucial role on the regeneration of the solar magnetic field. Among other layers, we should point out the tachocline, the base of the convection zone, and the super-adiabatic layer.

The density profile considered in the computation of the magnetic field under the approximation of the axisymmetric dynamo model follows a polytropic power law (Equation (3)), which ignores most of the complex density variations related with the microscopic and macroscopic variations of the solar plasma, namely in the tachocline layer and in the super-adiabatic region. This density profile (Equation (3)) is quite different from the density $\rho_{\rm ssm}(r)$ obtained from the standard solar model.

Figure 2 shows the relative difference between the polytropic density $\rho_{\rm pol}(r)$ and the $\rho_{\rm ssm}(r)$ in the layers where the solar dynamo is taking place, i.e., beneath the base of convection zone and the solar envelope. $\rho_{\rm ssm}(r)$ is almost similar for both solar chemical compositions (AGS05 or GS98), although there are a few differences in the base of the convective zone. The density difference for both abundances in certain layers is very significant, namely, in the tachocline layer and near the surface, more exactly, in the super-adiabatic region. These are also the regions where the solar magnetic field is continuously destroyed and regenerated.

To test the importance of the density stratification on the formation and evolution of the solar magnetic cycle, the polytropic density $\rho_{\rm pol}(r)$ used in the solar dynamo was replaced by the density profile $\rho_{\rm ssm}(r)$. Accordingly, the stream function $\Psi(r, \theta)$ was modified to accommodate $\rho_{\rm ssm}(r)$. This alteration was done in all the regions where the dynamo is operating, $R_{\rm b} \leqslant r \leqslant R_{\rm t}$ or $0.55\ R_\odot \leqslant r \leqslant R_\odot$. We note that, unlike $\rho_{\rm pol}(r)$, $\rho_{\rm ssm}(r)$ shows a variation of several orders of magnitude from 10^{-1} g cm^{-3} up to 10^{-7} g cm^{-3}.

For that reason, we choose to use in the dynamo models the solar density profile $\rho_{\rm ssm}(r)$ obtained from a standard model with the solar composition of GS98. The new stream function

Table 1
Solar Dynamo Models

Model	R_t[a] ($R_\odot$)	T[b] (yr)	$B_{\rm rs}$[c] (G)	Angle[d] (deg)
Polytropic	1.00	13.3	2950	40°
A	0.96	14.3	2750	30°
B	0.97	15.6	2400	20°
C	0.98	18.6	2000	10°
D	0.99	24.1	1360	<10°
D*	0.99	27.0	2640	40°
E	1.00	74.0	200	40°

Notes.
[a] R_t—external layer of the solar dynamo model.
[b] T—the half-period of the magnetic cycle.
[c] $B_{\rm rs}$—the magnitude of the radial component of the magnetic field at the surface.
[d] Angle of maximum de-placement of the magnetic field by eruption at the surface.

$\Psi_{\rm ssm}(r, \theta)$ was defined in such a way that the main properties of the reference dynamo model are maintained. $\Psi_{\rm ssm}(r, \theta)$ is given by

$$\Psi_{\rm ssm} = \Psi_{\rm pol} + \epsilon(r)\Psi_{\rm pol}, \quad (4)$$

with $\epsilon(r) = (\rho_{\rm ssm}(r) - \rho_{\rm pol}(r))/\rho_{\rm pol}(r)$. This stream function was chosen such that the meridional circulation of the new dynamo model (with new $\rho_{\rm ssm}(r)$) is identical to the meridional circulation of the reference dynamo model, i.e., $v_r(\Psi_{\rm ssm})$ is identical to $v_r(\Psi_{\rm pol})$.

In the following, we compute a succession of solar dynamo models (using the new stream function $\Psi_{\rm ssm}$) for a different external boundary $R_{\rm t}$ (see Table 1). Furthermore, all theses models have the same maximum velocity (at mid-latitude) of 25 m s^{-1} in the surface, and the same cutoff values for the turbulent diffusivity, with the exception of dynamo model E. In this last model, we have changed other parameters of the dynamo model to be able to maintain the same velocity at mid-latitude. It is worth noticing that for model E, R_t is equal to $R_\odot$, a location where the value of $\rho_{\rm ssm}$ is very small, and consequently the toroidal and poloidal components of the diffusivity must be reduced to compensate for such a dramatic variation of $\Psi_{\rm ssm}$. We found that a stable periodic solution of the magnetic field can be found if $\eta_{\rm to} = 5.0 \times 10^9$ cm^2 s^{-1} and $\eta_{\rm po} = 5.0 \times 10^{10}$ cm^2 s^{-1}. The coefficients are the same for $\rho_{\rm ssm}$ obtained with any of the solar compositions.

Figure 3 shows the difference between the components of the meridional circulation of the new dynamo models and the reference dynamo model. The v_r and v_θ components show variations between dynamo models mainly related with the choice of $R_{\rm t}$. More significantly, the v_θ component shows variations that are related with the peculiarities of the new density profile in several regions of the solar envelope, especially in the super-adiabatic layer.

5. THE BUTTERFLY DIAGRAM

Our reference dynamo model has a half-magnetic cycle period of 13.3 years which is slightly larger than the expected 11 years of the averaged solar magnetic cycle. As usual, we consider that the solar magnetic cycle in the dynamo model is considered to be equal to the period of the toroidal component of the magnetic field at the base of the convective zone (cf. Figure 4). Table 1

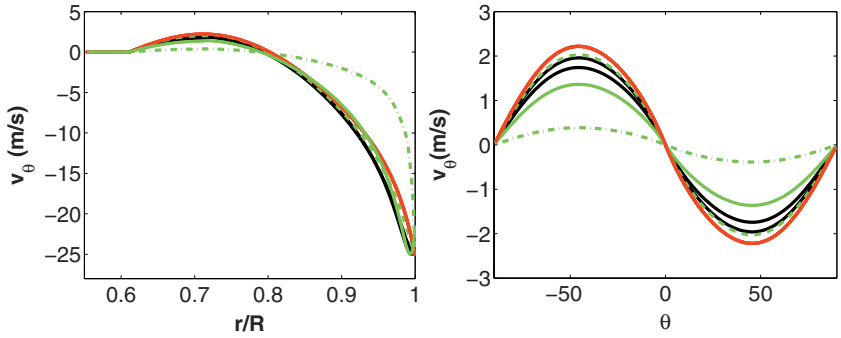

Figure 3. Variation of the component of the meridional circulation v_θ (m s^{-1}) with radius at mid-latitudes (left panel), and with the latitude at the lower limit of the tachocline (right panel). v_θ (m s^{-1}) is shown for the reference dynamo model (red line), as well as for several dynamo models (with the density profile $\rho_{\rm ssm}(r)$): A (0.96 $R_\odot$, dashed green line), B (0.97 $R_\odot$, continuous black line) and C (0.98 $R_\odot$, continuous black line), D(0.99 $R_\odot$, continuous green line), and E($R_\odot$, dash-dotted green line). The reference dynamo model was computed within an envelope, $R_b = 0.55\ R_\odot$ and $R_{\rm t} = R_\odot$. In the case of dynamo models with the density profile $\rho_{\rm ssm}(r)$, the value $R_{\rm t}$ was chosen as indicated previously (see the main text for details).

(A color version of this figure is available in the online journal.)

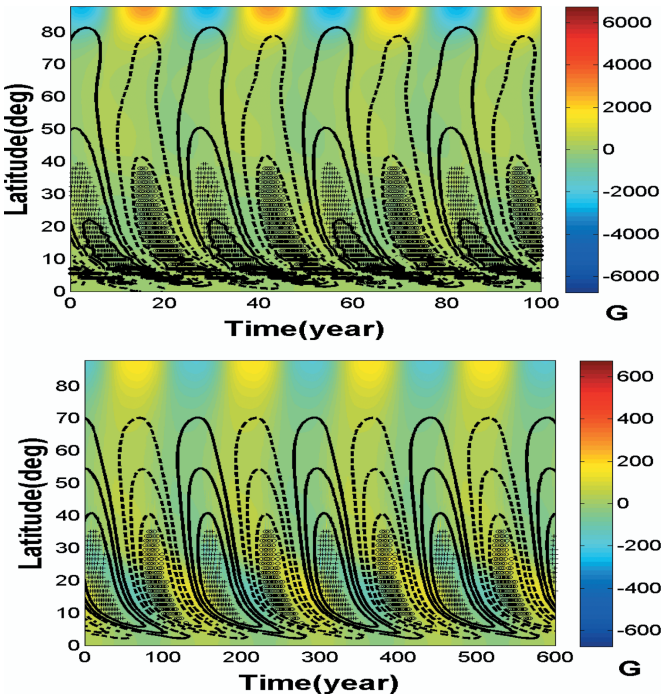

Figure 4. Magnetic field evolution for the reference dynamo model ($\Psi_{\rm ref}$—polytropic density profile $\rho_{\rm pol}$) and a dynamo model with a realistic density profile ($\Psi_{\rm ssm}$—solar/helioseismology density profile $\rho_{\rm ssm}$ for solar model GS98—model E). Both models have been calibrated to have a $v_0 = 25$ m s^{-1} at the Sun's surface. The color scale shows the radial surface magnetic field with negative and positive values shown as blue and red colors (the intensity of the field is expressed in gauss). The contours show the positive (continuous lines) and negative (dashed lines) values of the magnetic field at the base of the convective zone. The butterfly diagram of latitudinal eruptions is shown as "o" and "+" data points, indicating negative and positive values of the magnetic field that arrives at the surface.

(A color version of this figure is available in the online journal.)

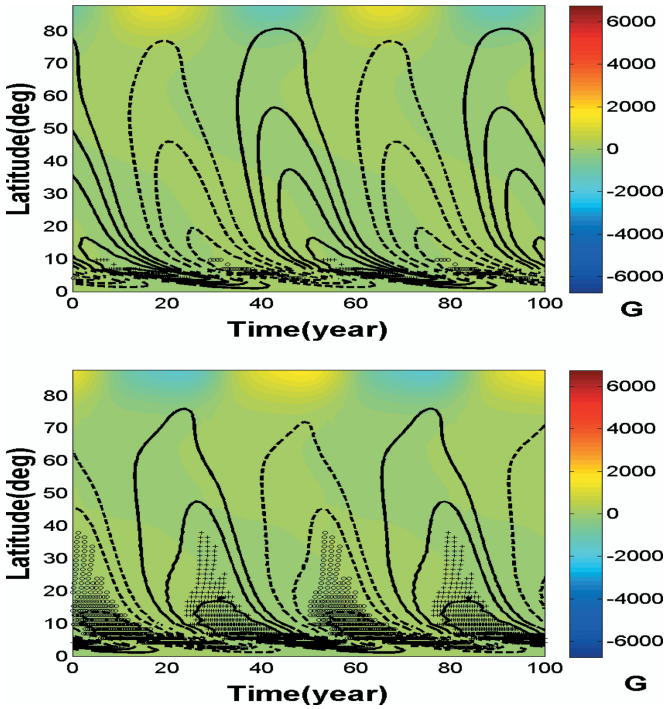

Figure 5. Magnetic field evolution for a dynamo model with a realistic density profile ($\Psi_{\rm ssm}$—solar/helioseismology density profile $\rho_{\rm ssm}$ for solar model GS98) and with $R_{\rm t} = 0.99\ R_\odot$ (model D; top panel) and $R_{\rm t} = 0.99\ R_\odot$ (model D* modified; bottom panel). Both models have been calibrated to have a $v_0 = 25$ m s^{-1} at the Sun's surface. The color scheme is the same as used in Figure 4.

(A color version of this figure is available in the online journal.)

presents the results of several other models with different values of R_t.

The difference between consecutive dynamo models A-to-D follows from the progressive decrease v_θ between R_p and the position of the return flow approximately at 0.80 $R_\odot$ (cf. Figure 3), which is more pronounced in the case of v_θ as a function of the latitude rather than v_θ as a function of the radius. Furthermore, we found that an increase of the magnetic field could be obtained if we reduce the total magnetic diffusivity by a convenient choice of parameters, as can be seen in Table 1. In the case of model D* (modified), for which $\eta_{\rm to}$ is reduced to 1×10^{10} cm^2 s^{-1}, the magnetic field reaches a latitude of 40° with a half-magnetic period of 27 years (cf. Figure 5). In this model, the magnitude of the polar magnetic field at the surface is 10% of the value of dynamo model of reference. Another interesting feature in such model is the enlargement of the sunspot area with a strong asymmetry when compared with the previous dynamo models.

We discuss the dynamo model E independent of the other models, because the physical variation is somehow more

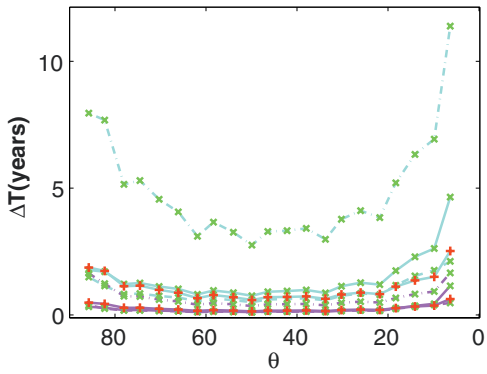

Figure 6. Interval of time traveled by a magnetic field element in a function of latitude, at the lower limit of the tachocline (cyan color) and near the surface (at approximately 0.94 $R_\odot$; magenta color). The dynamo models shown as the following ones: model of reference (red plus), solar model GS98 (green cross), dynamo model A (dashed line), dynamo model E (dashed point line), and dynamo model D (continuous line).

(A color version of this figure is available in the online journal.)

complicated, due to the complex structure of the very upper layers of the Sun's surface. By making this choice, we test the validity of this dynamo model to better understand its limitations. The density profile of the standard solar model present at the surface, $r = R_\odot$, shows a large magnitude variation when compared with the value of the density at $r = 0.99\ R_\odot$. As a consequence, the v_θ (as a function of radius or latitude) of model E ($R_t = R_\odot$) is very different from previous models, for example, model D (cf. Figure 3). Consequently, to obtain a steady and periodic solution for the solar dynamo for $v_0 = 25$ m s^{-1}, we had to change the cutoff of the turbulent magnetic diffusion (for the poloidal and toroidal components), η_{to} is reduced to 5×10^9 cm^2 s^{-1}, and η_{po} is reduced to 5×10^{11} cm^2 s^{-1}. Although the dynamo model E has a period duration of 74 years, the high latitude surface radial magnetic field is of the order of 200 G, similar to the model of Dikpati & Charbonneau (1999) and much closer to the value of 10 G estimated from observations.

We found that in such new dynamo models, the period of the magnetic cycle is regulated by the magnitude of the meridional counterflow at the base of the convective zone, which is consistent with the work of Muñoz-Jaramillo et al. (2010). The variation of the total magnetic diffusivity in model D shows that an increase of the period of the magnetic cycle, and an increase of the magnitude of the toroidal component of the magnetic field in the convection zone, was caused by the interplay between the advection and the diffusion. Furthermore, we also found that the increase in the magnitude of the toroidal field in the lower convective zone causes a slight increase of the poloidal component of the magnetic field produced at the surface, similar to what was found in the dynamo simulations of Dikpati (2011).

Figure 6 shows the averaged time interval for the displacement of the magnetic field from a latitude of 80° to a latitude of 0° (equator), two specific layers, one in the lower limit of the tachocline and a layer near surface (see Table 2). In the case of model E, the magnetic field takes 109.19 years (in the lower limit of the tachocline) and 16.34 years (near the surface) to progress between the two latitudes, these values are in strong contrast with the reference dynamo model, in which the values are 24.04 years (in the lower tachocline) and 5.98 years (near the surface).

Similarly, we obtained a reduction of the period duration of all the dynamo models relative to the model of reference.

Table 2
Time Interval Travel by the Magnetic Field

Model	T_{LRT}[a] (yr)	T_S[b] (yr)	$T^\star_{LRT}$ (%)	$T^\star_S$ (%)
Polytropic	24.04	5.98	...	...
A	20.25	4.53	−15.79	−24.39
B	20.93	4.32	−12.94	−27.83
C	23.54	4.44	−2.130	−25.80
D	30.14	5.14	25.36	−14.08

Notes.
[a] T_{LRT}—time interval at limit of the tachocline; $T^\star_{LRT}$ variation of T_{LRT} in relation to the reference (polytropic) solar dynamo model.
[b] T_S—time interval at surface; $T^\star_S$ variation of T_S in relation to the reference (polytropic) solar dynamo model.

The computation of dynamo models with density profiles using different abundances (GS98 and AGS05) leads to almost indistinguishable results. The function $\epsilon(r)$ (and $|d\epsilon(r)/dr|$) is identical to both density profiles, the exception being at the base of the convection zone for which GS98 abundance composition produces a deeper base of convection zone than the AGS05 abundance composition (see Figure 2). Nevertheless, this has a minor effect on the evolution of the solar magnetic cycle. The $\rho(r)$ computed with the AGS05 abundance composition increases the period of the magnetic cycle of models of A, B, C, and D by 3% to 14.7, 16.1, 19.4, and 24.8 compared to dynamo models for which $\rho(r)$ was computed using the GS98 abundance composition. The maximum magnetic field occurs at similar latitudes for both density profiles (GS98 and AGS05) and approximately the same amplitude on both the components. We also found from analyzing the dynamo models A-to-D that the tachocline has a stronger influence in the period of the magnetic cycle when compared with the case of the reference solar dynamo (see Table 2). In model D (see Table 2), the time interval relatively to the model of reference increases 25% as opposed to other models. This is consistent with the results presented in Figure 6.

6. SUMMARY AND CONCLUSION

The impact of the stratification density on the solar dynamo could only be fully addressed by a self-consistent magnetic-hydrodynamic numerical simulation of the magnetic field acting in the Sun's envelope, from below the convection zone up to the upper-adiabatic layer. In particular, helioseismology has shown that the magnetic field and the differential rotation can visibly modify the structure of the upper layers of the Sun. Unfortunately, the modeling of such physical process is very complex. In this work, this problem was addressed in an indirect way, by taking advantage of the fact that the contribution of dynamical processes for the evolution of the Sun need to be relatively small (e.g., Turck-Chieze & Couvidat 2011). Preliminary studies of incorporating dynamical processes in the stellar evolution such as the differential rotation have been shown to have a small impact on the present structure of the Sun. This result is confirmed by the helioseismology analysis (e.g., Turck-Chieze et al. 2010).

The solar axisymmetric dynamo model has been a powerful tool in studying a diversity of properties of the solar magnetic cycle. In such types of dynamo models, the meridional flow is computed under the assumption that the stratification of the convection zone follows a polytropic stratification (in this work,

we called it the reference solar dynamo model). Unfortunately, the polytropic stratification presents several shortcomings, this description of the solar envelope is unable to represent properly the complex structure of the upper layers of the Sun and of layers beneath the base of convection zone. A problem common to many other dynamo computations.

In this preliminary work, we investigated the impact that a more realistic stratification (density profile) has on such a type of solar dynamo. This was done by replacing the polytropic density profile by a more realistic density profile obtained from the standard solar model, which is in itself consistent with helioseismology. We investigate how this density profile affects the evolution of the solar magnetic cycle.

We found that, if the new solar dynamo model is restricted to a region between 55% and 96% of the solar radius, then the butterfly diagram of such a dynamo model is similar but not equal to the butterfly diagram of the reference solar dynamo. In this case, the difference between dynamo models is due to the different density stratification beneath the base of the convection zone, a region which plays an important role in the regeneration of the solar magnetic cycle. The solar dynamo models that take into account the density profile above $0.96\,R_{\odot}$ have a quite different butterfly diagram, caused by a dramatic change in the strength of the poloidal and toroidal components of magnetic fields, and a significant increase of the period of the solar magnetic cycle. This clearly establishes the importance of the external layers in the evolution of the solar magnetic cycle. In particular, the sunspots latitude distribution shows an asymmetric pattern that is in qualitative agreement with observations (cf. Figure 4). Finally, the chemical composition (AGS05 or GS98) of the standard solar model leads to distinct solar density profiles when compared with helioseismology data. However, the impact of such density difference does not significantly affect the strength of the magnetic field and the time duration of the magnetic cycle.

In general, we found that the main properties of the solar magnetic cycle are maintained. This shows that the applicability of this type of dynamo model is larger than previously thought, despite the fact that the upper layers of the Sun have a very complex structure.

Finally, it is worth mentioning that the inclusion of a more realistic density in the reference solar model must be considered in future work, once its impact on the evolution of the solar magnetic cycle is larger than other dynamical processes usually included in the reference dynamo model. Furthermore, we believe that much can be gained from a stronger interaction between the research groups of the solar dynamo and the modeling of the Sun as a star, not only to understand the features behind the solar dynamo, but also to properly introduce into the solar evolution models the dynamical processes related to the magnetic field, which play a crucial role in the evolution of our star.

This work was supported by a grant from "Fundação para a Ciência e Tecnologia." We also thank the authors of solar dynamo code SURYA for making their code available to the public. We acknowledge the suggestions and comments by the anonymous referee, which have significantly contributed to improve the presentation of our work.

REFERENCES

Asplund, M., Grevesse, N., & Sauval, A. J. 2005, in ASP Conf. Ser. 336, Cosmic Abundances as Records of Stellar Evolution and Nucleosynthesis in Honor of David L. Lambert, ed. T. G. Barnes, III & F. N. Bash (San Francisco, CA: ASP), 25
Asplund, M., Grevesse, N., Sauval, A. J., & Scott, P. 2009, ARA&A, 47, 481
Babcock, H. W. 1961, ApJ, 133, 572
Bahcall, J. N., Serenelli, A. M., & Basu, S. 2005, ApJ, 621, L85
Basu, S., Chaplin, W. J., Elsworth, Y., New, R., & Serenelli, A. M. 2009, ApJ, 699, 1403
Bonanno, A., Elstner, D., Rüdiger, G., & Belvedere, G. 2002, A&A, 390, 673
Charbonneau, P. 2010, Living Rev. Sol. Phys., 7, 3
Charbonneau, P., Christensen-Dalsgaard, J., Henning, R., et al. 1999, ApJ, 527, 445
Chatterjee, P., Nandy, D., & Choudhuri, A. R. 2004, A&A, 427, 1019
Choudhuri, A. R., Chatterjee, P., & Jiang, J. 2007, Phys. Rev. Lett., 98, 131103
Choudhuri, A. R., Nandy, D., & Chatterjee, P. 2005, A&A, 437, 703
Choudhuri, A. R., Schüssler, M., & Dikpati, M. 1995, A&A, 303, L29
Dikpati, M. 2011, ApJ, 733, 90
Dikpati, M., & Charbonneau, P. 1999, ApJ, 518, 508
Dikpati, M., & Choudhuri, A. R. 1995, Sol. Phys., 161, 9
Dikpati, M., & Gilman, P. A. 2012, ApJ, 746, 65
Durney, B. R. 1997, ApJ, 486, 1065
Grevesse, N., & Sauval, A. J. 1998, Space Sci. Rev., 85, 161
Guerrero, G., & de Gouveia Dal Pino, E. M. 2008, A&A, 485, 267
Guzik, J. A. 2011, Ap&SS, 336, 95
Guzik, J. A., & Mussack, K. 2010, ApJ, 713, 1108
Haber, D. A., Hindman, B. W., Toomre, J., et al. 2002, ApJ, 570, 855
Hathaway, D. 2011, arXiv:1103.1561
Howe, R. 2009, Living Rev. Sol. Phys., 6, 1
Krause, F., & Raedler, K.-H. 1980, Mean-field Magneto hydrodynamics and Dynamo Theory (Oxford: Pergamon)
Leighton, R. B. 1969, ApJ, 156, 1
Lopes, I. P., & Gough, D. 2001, MNRAS, 322, 473
Lopes, I., & Passos, D. 2009, Sol. Phys., 257, 1
Mitra, D., Moss, D., Tavakol, R., & Brandenburg, A. 2011, A&A, 526, A138
Moffatt, H. K. 1978, Magnetic Field Generation in Electrically Conducting Fluids, ed. G. K. Batchelor & J. W. Miles (Cambridge: Cambridge Univ. Press)
Morel, P. 1997, A&AS, 124, 597
Muñoz-Jaramillo, A., Nandy, D., & Martens, P. C. H. 2009, ApJ, 698, 461
Muñoz-Jaramillo, A., Nandy, D., & Martens, P. C. H. 2011, ApJ, 727, L23
Muñoz-Jaramillo, A., Nandy, D., Martens, P. C. H., & Yeates, A. R. 2010, ApJ, 720, L20
Nandy, D., & Choudhuri, A. R. 2001, ApJ, 551, 576
Nandy, D., & Choudhuri, A. R. 2002, Science, 296, 1671
Nordlund, Å., Stein, R. F., & Asplund, M. 2009, Living Rev. Sol. Phys., 6, 2
Passos, D., & Lopes, I. 2012, MNRAS, 422, 1709
Rempel, M. 2006, ApJ, 647, 662
Rosenthal, C. S., Christensen-Dalsgaard, J., Houdek, G., et al. 1995, in Proc. 4th SOHO Workshop: Helioseismology, Seismology of the Solar Surface Regions, ed. J. T. Hoeksema et al. (ESA SP-376; Noordwijk: ESTEC), 459
Rosenthal, C. S., Christensen-Dalsgaard, J., Nordlund, Å., Stein, R. F., & Trampedach, R. 1999, A&A, 351, 689
Schou, J., Antia, H. M., Basu, S., et al. 1998, ApJ, 505, 390
Serenelli, A. M., Basu, S., Ferguson, J. W., & Asplund, M. 2009, ApJ, 705, L123
Turck-Chieze, S., Basu, S., Brun, A. S., et al. 1997, Sol. Phys., 175, 247
Turck-Chieze, S., & Couvidat, S. 2011, Rep. Prog. Phys., 74, 6901
Turck-Chieze, S., & Lopes, I. 1993, ApJ, 408, 347
Turck-Chieze, S., Palacios, A., Marques, J. P., & Nghiem, P. A. P. 2010, ApJ, 715, 1539
Yeates, A. R., Nandy, D., & Mackay, D. H. 2008, ApJ, 673, 544
Zhao, J., & Kosovichev, A. G. 2004, ApJ, 603, 776